Sliding spin-density wave in $(TMTSF)_2PF_6$ studied with narrow-band noise

Tomoyuki Sekine,* Norikazu Satoh, and Mitsuhiro Nakazawa
Department of Physics, Sophia University, 7-1 Kioi-cho, Chiyoda-ku, Tokyo 102-8554, Japan

Toshikazu Nakamura
Institute for Molecular Science, Myodaiji, Okazaki 444-0867, Japan
(Received 10 March 2004; revised manuscript received 30 June 2004; published 3 December 2004)

We report narrow-band noise (NBN) due to sliding motions of the spin-density wave (SDW) condensate at 2.0 K in three samples of $(TMTSF)_2PF_6$ and the magnetic-field effects. Typical NBN spectra coming from the saw-toothed-wave current oscillations are clearly observed. The periodic peaks due to the $4k_F$-charge-density wave (CDW) collective excitation are found, together with the SDW moving with a faster velocity, revealing that the sliding mode of the SDW is coupled with $4k_F$-CDW fluctuations. Observation of the interference peaks gives evidence of spatially nonuniform dc current carried by the deformable SDW in domains. At large currents the NBN spectrum drastically changes with increasing current and depends on applied magnetic field, suggesting a dynamical phase transition from the plastic-flow phase to the moving-solid phase. In the moving-solid phase the frequencies of the periodic peaks decrease with increasing current because the spatial coherency grows rapidly. The current oscillations in this phase are interpreted in terms of the coexistence of the $2k_F$-CDW collective excitation with the phason.

DOI: 10.1103/PhysRevB.70.214201 PACS number(s): 71.45.−d, 72.15.Nj, 75.30.Fv

I. INTRODUCTION

The Peierls instability of the Fermi surface drives the one-dimensional conductor to a metal-insulator transition accompanied by a formation of the density wave. One fascinating aspect of the density waves is the possibility of carrying a current by the collective motions of the density wave. Dynamics of the collective motions has been extensively studied, since the discovery of the nonlinear electrical response due to the sliding charge-density wave (CDW) in $NbSe_3$.[1] Below the threshold electric field E_T, the density wave is pinned by impurities and the electric current is transported by normal carriers thermally excited above the Peierls gap. When the electric field E exceeds E_T, the density wave slides and gives a nonlinear contribution to the electric current. In other words, a low-energy collective mode in the density wave, which is related to the spatial variations of the phase and is called phason, plays a crucial role in the nonlinear conductivity.

The sliding motions of the spin-density wave (SDW) condensate were first observed in the quasi-one-dimensional organic conductor $(TMTSF)_2NO_3$ by Tomić *et al.*[2] They found that the conductivity parallel to the one-dimensional a axis increased above E_T. Later, the nonlinear conductivity due to the sliding motions of the SDW condensate was studied also in $(TMTSF)_2PF_6$.[3,4]

Simultaneously the narrow-band noise (NBN) originating from the current oscillations with a fundamental frequency f given by

$$f = \frac{J_{\mathrm{SDW}}}{en_{\mathrm{SDW}}\lambda_{\mathrm{pin}}}, \tag{1}$$

appears in the sliding SDW state when the correlation length is enough long. Here, J_{SDW} is the current density, n_{SDW} the density of condensed electron, and λ_{pin} the effective pinning length. It was actually observed in $(TMTSF)_2ClO_4$,[5,6] $(TMTSF)_2AsF_6$,[7] and $(TMTSF)_2PF_6$.[8] However, the reported NBN spectra are not distinct when compared with those of CDW.[9] Moreover, the Shapiro interference between the current oscillations and the applied ac field was observed in $(TMTSF)_2AsF_6$ when the ac electric field was externally applied under the bias of dc voltage greater than E_T.[7] Within the framework of these observed experimental results, the sliding motions of the SDW are very similar to those of the CDW and understood by the classical depinning mechanism.

Recently, the coexistence of SDW with $2k_F$ and $4k_F$ CDWs was found between 4 and 12 K in $(TMTSF)_2PF_6$ by x-ray diffraction measurements,[10–12] where $\boldsymbol{k}_F$ is the Fermi wave vector and was evaluated to be $0.5\boldsymbol{a}^* + 0.24\boldsymbol{b}^* - 0.06\boldsymbol{c}^*$ by NMR.[13] Here, $\boldsymbol{a}^*$, $\boldsymbol{b}^*$, and $\boldsymbol{c}^*$ denote the reciprocal lattice vectors. The coexistence of $2k_F$ CDW with SDW was explained theoretically in terms of the next-nearest-neighbor Coulomb interaction, while the nearest-neighbor interaction induces the $4k_F$ CDW.[14–16] In the coexistent state of $2k_F$ SDW and $2k_F$ CDW the electron densities $n_\uparrow$ with up spins and $n_\downarrow$ with down spins are, respectively, written as

$$n_\uparrow = A_\uparrow \sin(2\boldsymbol{k}_F \cdot \boldsymbol{r} + \theta + \phi), \tag{2}$$

and

$$n_\downarrow = -A_\downarrow \sin(2\boldsymbol{k}_F \cdot \boldsymbol{r} + \theta - \phi). \tag{3}$$

A pure SDW corresponds to $n_\uparrow - n_\downarrow$, with the two waves out of phase ($\phi = 0$) when the amplitudes of the two waves are the same as each other ($A_\uparrow = A_\downarrow$). A coexistent SDW-CDW state is obtained for an arbitrary phase shift 2ϕ between $n_\uparrow$ and $n_\downarrow$ when $A_\uparrow = A_\downarrow$. For the collective modes of this coexistent SDW-CDW state the dynamical part of phase θ gives rise to the sliding motion, i.e., a phason, and the dynamical part of ϕ represents the relative motion of the density wave

with opposite spins followed by amplitude of the $2k_F$ CDW. In this state, not only a phason mode but also a CDW collective mode originating from the fluctuations of ϕ has low energy at the boundary region between pure SDW state and the coexistent SDW-CDW one.[17,18] Furthermore, it has been theoretically pointed out that the phase mode at long wavelength is coupled with the $4k_F$-CDW fluctuations in the one-dimensional quarter-filled SDW states.[17–19]

Then, it is expected that the low-energy CDW collective modes also contribute to the nonlinear conduction and the NBN in the SDW state, but this has not been observed yet. In this work, we measure the NBN in the SDW state of the quasi-one-dimensional organic conductor $(TMTSF)_2PF_6$ with a quarter-filled band to study the collective excitations and the magnetic-field effects on them.

II. EXPERIMENT

Single crystals were synthesized with the standard electrochemical growth method. The standard four-probe method was applied to the NBN measurements. The current probe contacts were attached onto the *a* crystal planes with gold wires of 20 μm diameter by gold paint, and the distance between voltage contacts, with which the following results were obtained, was 0.2–0.5 mm. The samples were cooled at a rate of about 0.3 K/min in order to avoid the irreversible resistance jump. The SDW transition was clearly observed at about 12 K by measuring resistance on the cooling process. The temperature was kept at 2.0 K within ±0.02 K by cooling the samples with a stream of cold helium gas and at 4.2 K by immersing them in liquid He in the NBN measurements. We measured the NBN spectra under various constant electric currents at 2.0 and 4.2 K by using a spectrum analyzer (Anritsu, model MS420B). It is available between 10 Hz and 30 MHz. The magnetic field H was applied along the b' direction using a superconducting magnet (Oxford, Teslatron).

III. RESULTS

We show typical NBN spectra in three samples.

Figure 1 shows the current-voltage characteristics observed at 2.0 K in samples P32, P55, and P56. In sample P32, the nonlinear part of the current very rapidly increased above a definite threshold electric field E_T, and consequently the threshold voltage V_T was clearly observed. We obtain that $V_T \cong 0.32$ V at 0 T and 0.41 V at 10 T in sample P32. On the other hand, the threshold voltage of samples P55 and P56 cannot be easily read from this figure. Then, we also show their conductance as a function of current in the inset. We obtain that $V_T \cong 0.03$ V in sample P56 and 0.02 V in sample P55. But, these results of samples P55 and P56 are problematic, which will be discussed later. Next, let us discuss the NBN spectra of these samples.

A. NBN in sample P56

Figure 2 shows the NBN spectra at 2.0 K and $H=0$ T in sample P56. No periodic peak was detected below 0.2 mA. The baselines of the NBN spectra lie at about −140 dB.

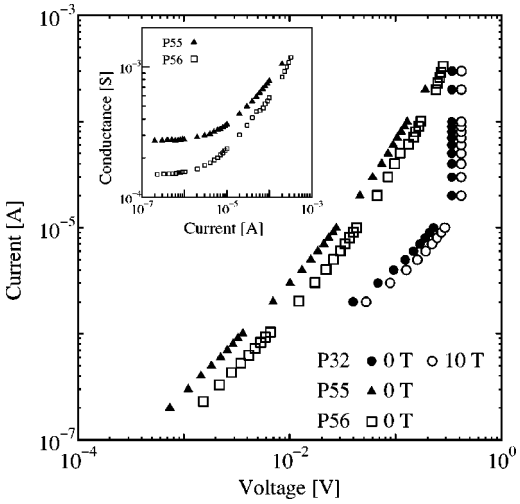

FIG. 1. Current-voltage characteristics at 2.0 K in samples P32, P55, and P56. The inset shows the conductance of samples P55 and P56 as a function of current.

When the applied voltage was about ten times greater than V_T, i.e., above 0.25 mA, we clearly observed periodic peaks, whose periodicity increased with increasing current. The NBN spectra observed in sample P56 are almost the same ones as reported frequently in the CDW states of the one-dimensional conductors.[9,20] We call it "stick-slip noise." The observed NBN spectra are much clearer than those reported by Hino *et al.*[8]

Figure 3 shows the frequencies of the periodic peaks in the NBN as a function of current. The fundamental frequency and its harmonic frequencies seem to appear at a finite current I_T^0, contrary to Eq. (1). The I_T^0(=0.237 mA) is much larger than the threshold current (~0.01 mA) esti-

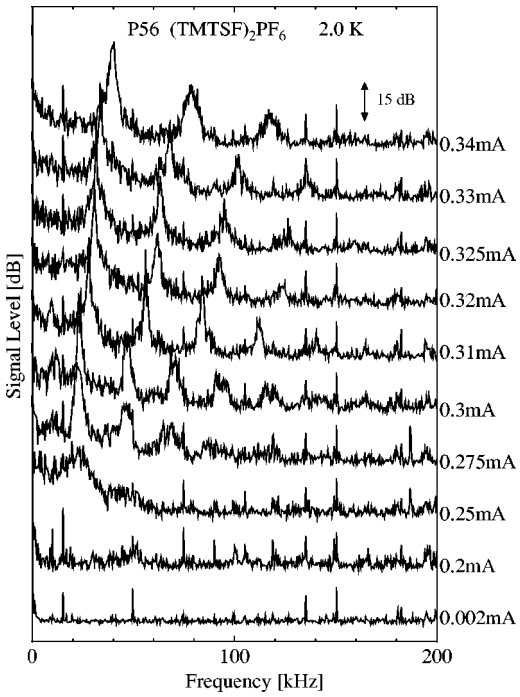

FIG. 2. NBN spectra of sample P56 at 2.0 K when $H=0$ T.

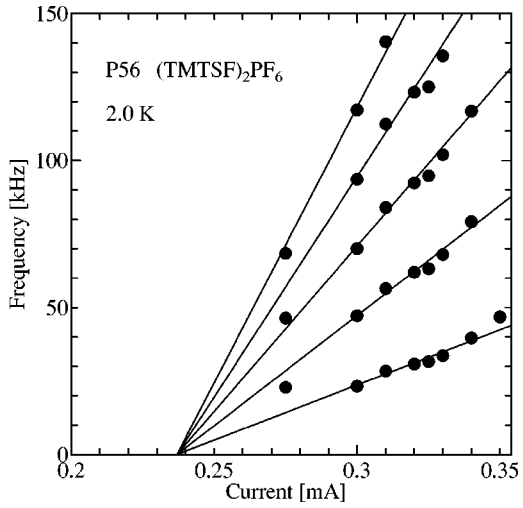

FIG. 3. The frequencies F of the periodic peaks as a function of current in sample P56. Solid lines denote $F=\ell f=375\ell(I-0.237)$kHz, where I is scaled in mA and $\ell=1$, 2, 3, 4, and 5.

mated from Fig. 1. The crystal of sample P56 was probably cracked in the cooling process from room temperature. Although the cracking partly shuts current path off in a part of the one-dimensional linear chains, it also shunts current path, because the cracks occur along the linear chain. Thus, the whole current flows dividedly in separated paths. Then, the resistance R_0, parallel to R of a part of the sample in which the NBN measurements were done practically in the circuit, should be taken into account, as shown in Fig. 4(a).

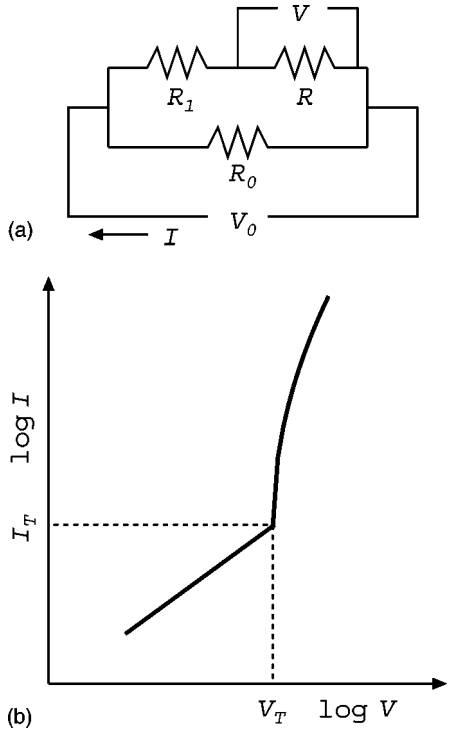

FIG. 4. (a) The equivalent circuit for the NBN measurements in the present samples and (b) the ideal current-voltage characteristic.

Consequently, the threshold voltage is observed to be dull in the $I-V$ curve. The excess current I_{SDW}, which is carried by the SDW condensate, is estimated by

$$I_{\mathrm{SDW}} = \alpha I - \frac{V}{R_n} \cong \alpha\left(I - \frac{I_T}{\alpha}\right), \tag{4}$$

where I is the total current supplied with a current source and R_n represents the ohmic-resistance part due to the normal carriers in the resistance R.[5] And, α is given as $R_0/(R_0+R_1+R)$, which depends on V_0 and V above the threshold electric field because of the inhomogeneity in sample. Here, V_0 is the voltage applied to the entire sample. If R_0 is infinite, the $I-V$ characteristic for the ideal sample may be described, as shown in Fig. 4(b), with a rapid increase of I_{SDW} above the threshold voltage. This behavior was observed in sample P32. A similar $I-V$ characteristic was observed also in the CDW system of $K_{0.3}MoO_3$.[9] Then, we may define the threshold current I_T. Assuming that the part of the sample with resistance R in which the NBN measurements were done is homogeneous for E_T and has the ideal $I-V$ characteristic, we may replace V/R_n by I_T, because I increases without a marked increase of the applied voltage. Actually, only one series of the sharp periodic peaks was observed and their frequencies linearly increase as a function of $(I-I_T^0)$, suggesting that the part of the sample in which the NBN measurements were done has a homogeneous threshold electric field E_T and the SDW with a long correlation length is formed in this part. In the NBN spectra of the inhomogeneous CDW systems[21–24] several series of the fundamental and harmonics were observed. When the homogeneity becomes worse, it may be difficult to observe the NBN spectrum. If the threshold electric field E_T^0 of the other part of the sample with resistance R_0 is lower than that (E_T) of the part with R, the total current I increases rapidly but V does not increase in proportion to I. Then, the conductance I/V obtained in the circuit of Fig. 4(a) seemingly increases when the electric field is between E_T^0 and E_T. Thus, the threshold becomes indistinct. Moreover, the observed threshold current $I_T^0=I_T/\alpha$ becomes very large, because R_0 and α decrease near E_T. We think that this happens on sample P56. In fact, the voltage V hardly increased when I is increased from 0.25 to 0.33 mA, as seen in Fig. 1, i.e., when the periodic peaks appeared. As will be mentioned later, on the other hand, sample P32 is considered to be very homogeneous all over the sample and its threshold current I_T^0 is very small.

The substantial cross section of the part of the sample in which the NBN measurements were done is approximately given as αS below E_T^0 and far above E_T. Here, S is the cross section of the entire sample. Assuming that α is independent of V and the substantial cross section is given as αS, we estimate that $\lambda_{\mathrm{pin}}=33$ Å by using $I_T^0=I_T/\alpha=0.237$ mA, $n_{\mathrm{SDW}}=1.40\times10^{21}$ cm^{-3}, and $S=3.6\times10^{-5}$ cm^2.

The SDW is pinned by nonmagnetic impurities in the second-order pinning process, which gives $\lambda_{\mathrm{pin}}=\lambda_{\mathrm{SDW}}/2$.[25] For magnetic impurities, the first-order pinning arises similarly to the CDW case, which gives $\lambda_{\mathrm{pin}}=\lambda_{\mathrm{SDW}}$. Assuming $\lambda_{\mathrm{pin}}=\lambda_{\mathrm{SDW}}\simeq 2a(\simeq 14.6$ Å), the present result is in agreement with λ_{SDW} but a little bit larger than it. Here, a is the lattice

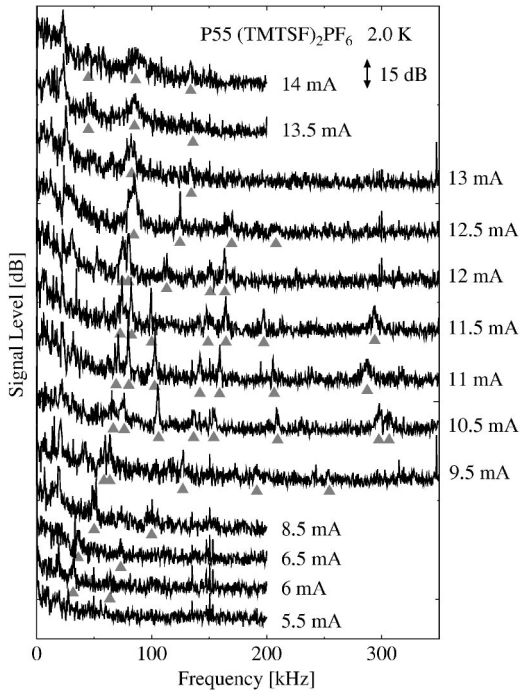

FIG. 5. NBN spectra of sample P55 at 2.0 K when $H=0$ T. Triangles denote the periodic peaks.

constant of the *a* axis in the normal state and only the component $k_{Fx}(\simeq \pi/2a)$ of the Fermi wave vector along the *a* axis was taken into account, since the currents flowed along the *a* axis. This discrepancy is probably due to the underestimation by giving the substantial cross section of the sample αS.

B. NBN in sample P55

Figure 5 shows the NBN spectra at 2.0 K in sample P55. We observed a fundamental peak and its harmonics at small currents above about 6 mA. They are very sharp when compared with the periodic peaks of sample P56. The frequencies of the periodic peaks are linearly proportional to $(I-I_T^0)$ except for the abnormal peaks, which will be discussed later. These facts suggest that the threshold electric field E_T is not distributed in the part of the sample in which the NBN was measured and the SDW with a long correlation length is formed in this part. On the other hand, we read the threshold current as 0.01 mA from the inset of Fig. 1. The currents where we observed the periodic peaks in the NBN spectra are much higher than the threshold current estimated from Fig. 1. We think that this can be explained by the equivalent circuit of Fig. 4, although we did not measure the $I-V$ characteristic in this current region, unfortunately.

The observed periodic peaks come from the stick-slip noise. In addition to them, several new peaks were found between $I_1'=9.0$ and $I_2'=12.0$ mA. The fundamental and its harmonic peaks split in two peaks, respectively. Simultaneously another abnormal peak and its harmonics, which have almost the same intensities as those of the stick-slip noise, appear and their frequencies decrease with increasing *I*. The frequency dependence upon *I* is quite unusual, i.e., it

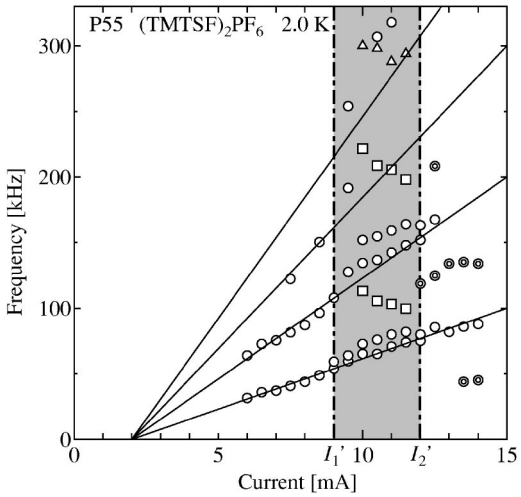

FIG. 6. The frequencies *F* of the periodic peaks as a function of current in sample P55. Solid lines denote $F=\ell f=7.69\ell(I-2.0)$kHz, where *I* is scaled in mA and $\ell=1$, 2, 3, and 4.

is contrary to Eq. (1). Usually the peak frequency of the NBN increases as the current *I* is increased, as seen in Figs. 2 and 3. The abnormal fundamental peak is split from the second harmonic peak of the stick-slip noise. Above $I_2'=12.0$ mA, the frequency of this fundamental of the abnormal peak turns to the opposite direction, i.e., it increases with increasing current. The frequency of the abnormal peak is approximately 1.5 times the fundamental frequency of the stick-slip noise. Moreover, we can see a weak peak whose frequency is one half of the fundamental frequency when $I=13.5$ and 14.0 mA, although the signal-to-noise ratio of the spectrum below 35 KHz was small. On the other hand, the pair of the fundamental seemingly joins into a close union as well as that of the second harmonic above I_2', but the combined peaks are broad.

The current dependence of the frequencies of the NBN spectra is shown in Fig. 6. The frequencies of the stick-slip noise are linear to I_{SDW}, assuming that $I_T^0=I_T/\alpha=2.0$ mA in Eq. (4). This suggests that the circuit in Fig. 3 is applicable to sample P55, as well as sample P56. Using the sample cross section $S=1.2\times10^{-3}$ cm^2, we estimate that $\lambda_{\mathrm{pin}}=48$ Å, which is roughly in agreement with $\lambda_{\mathrm{SDW}}\simeq 14.6$ Å.

In Fig. 6 one can clearly see that the abnormal fundamental peak and the second harmonic, which are denoted by squares, are split from the second and fourth harmonics of the stick-slip noise, respectively, although the fourth harmonic of the stick-slip noise was not observed. The third harmonic peak of the abnormal peak, which is denoted by a triangle in Fig. 6, was observed near 300 KHz, but its frequency is not perfectly equal to three times the fundamental frequency. Their frequencies decrease with increasing *I* between 10 and 11.5 mA. Moreover, the fundamental peak and the second harmonic one of the stick-slip noise, whose frequencies increase with increasing *I*, split in two peaks in this current region, respectively. The splitting strongly correlates with the appearance of the abnormal peak. The frequency of the low-frequency fundamental peak of the pair fits well with Eqs. (1) and (4), and then another high-frequency peak is regarded as a new peak.

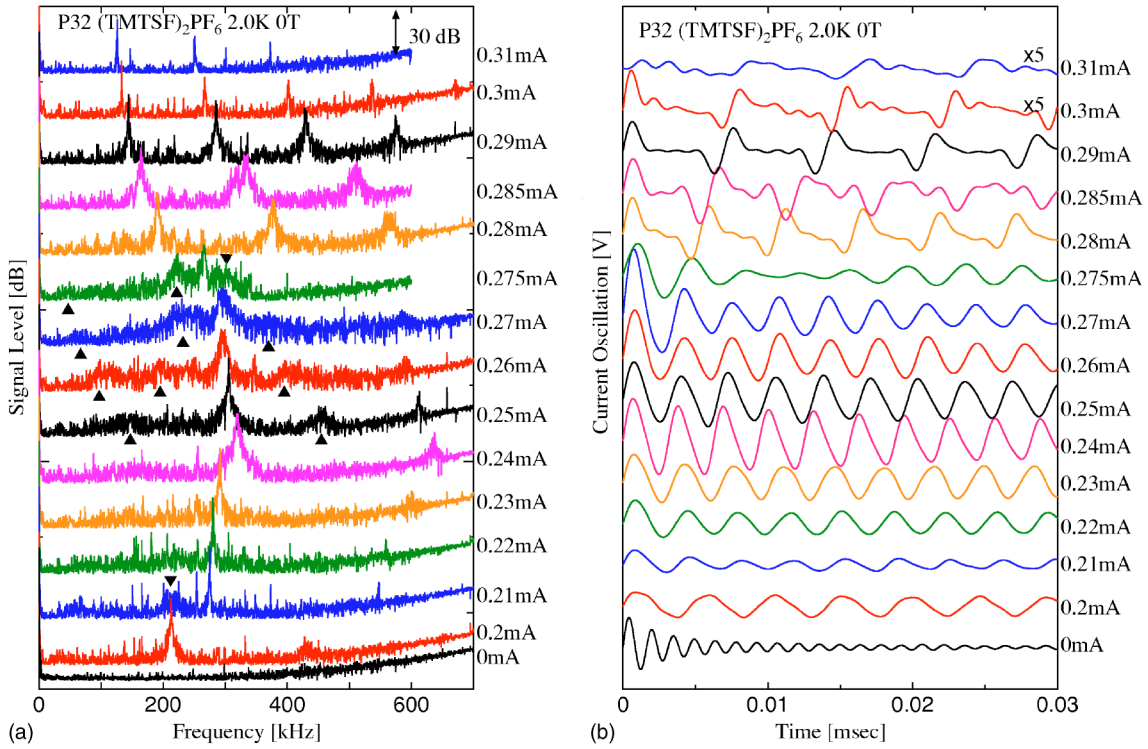

FIG. 7. (Color online) (a) NBN spectra of sample P32 at 2.0 K when $H=0$ T and (b) the current oscillations calculated by the inverse Fourier transformation. Triangles denote weak peaks. The current oscillations were obtained by subtracting that at 0 mA. The oscillation at 0 mA originates from the limited frequency region in the measurements.

Above I_2' the high-frequency peak seemingly was superimposed on the low-frequency peak, because the former peak, perhaps, broadened. Simultaneously the abnormal peak turned into $3/2$ times the fundamental frequency of the stick-slip noise in frequency, accompanying a weak peak at one half of the fundamental frequency. These are denoted by double circles in Fig. 6.

We also measured NBN spectra in this sample at 4.2 K, but we found no clear periodic peaks. This means that these periodic peaks in the NBN spectrum existed only near 2 K.

C. NBN in sample P32

Figure 7(a) shows the NBN spectra at 2.0 K and $H=0$ in sample P32. The periodic peaks were not detected at 0 mA, but these were observed just above the threshold voltage V_T. When compared with the results of samples P55 and P56, the observed NBN spectra are complicated and the peak frequency of the NBN is high, indicating that the SDW is sliding at a high speed. The spectra strongly depend on current I. The current oscillations were calculated by the inverse Fourier transformation, as shown in Fig. 7(b), assuming that the phases are zero. The frequencies of the periodic peaks as a function of current I are plotted in Fig. 8(a).

The periodic peaks are sharp when the current I is small and their frequencies increase with increasing I until $I_1 \simeq 0.245$ mA. The current oscillations exhibit the saw-toothed waves.

As shown in Fig. 1, the nonlinear part of the current very rapidly increased above V_T in sample P32. The differential conductivity dI/dV above V_T is enormous, and consequently the threshold voltage V_T was clearly observed in this sample. The excess current I_{SDW}, which is carried by the SDW condensate, is very sharply increased above V_T. Then, the frequencies of the observed periodic peaks linearly increase as a function of $I_{SDW}(=I-I_T^0)$ below $I_1 \simeq 0.245$ mA, as shown in Fig. 8(a). Here, we used the threshold current $I_T^0=I_T/\alpha$, which was estimated as 0.012 mA from the nonlinear $I-V$ curve in Fig. 1. The threshold current I_T^0 is very small in contrast with samples P55 and P56. The above-mentioned result and the $I-V$ curve indicate that the whole sample is homogeneous for the threshold electric field E_T and has a unique value of E_T all over the sample. Then, $\alpha(=R_0/(R_0+R_1+R))$ is independent of V_0 and V, i.e., constant, in contrast with the cases of samples P55 and P56.

The substantial cross section of the sample is nearly equal to αS in the homogeneous sample. Using the entire cross section $S=2.5\times10^{-4}$ cm^2, we estimate that $\lambda_{pin}=1.3$ Å, but it is much shorter than $\lambda_{SDW} \simeq 14.6$ Å. This is contrary to the cases of samples P56 and P55 in which the estimated λ_{pin} was larger than λ_{SDW}. We think that it comes from the intrinsic domain structure, which will be discussed later in detail.

The NBN spectrum broadens at 0.24 mA, just below I_1. At $I_1 \simeq 0.245$ mA $\leqslant I \leqslant I_2 \simeq 0.278$ mA the NBN spectra are complicated. One half of the fundamental periodicity appears weakly at 0.25 mA. At 0.26 mA several weak and broad nonperiodic peaks appear. Among them three peaks denoted by triangles are observed at about $f/3, 2f/3$, and $4f/3$, where f is the fundamental frequency of the strong periodic peaks. At $I=0.27$ and 0.275 mA a sideband is detected at $f \pm f'$

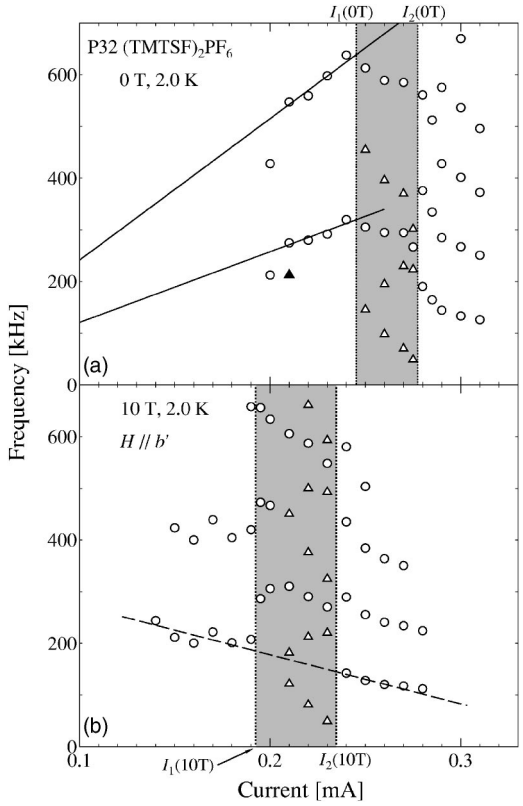

FIG. 8. The frequencies F of the strong periodic peaks (○) and the weak peaks (△) interfering with the periodic peaks in sample P32 as a function of I, (a) when $H=0$ T and (b) when $H=10$ T. Solid lines denote $F=\ell f=1370\ell(I-0.012)$kHz, where I is scaled in mA and $\ell=1$ and 2. A dashed line is drawn as a guide for the eyes. A closed triangle at $I=0.21$ mA denotes the remainder which was observed in the case of $I=0.2$ mA.

around the fundamental peak at f, and they seem to interact with each other. We also see a very weak and broad peak at f'. It is recognized that beats appear in the current oscillations at 0.27 and 0.275 mA ($\sim I_2$).

These facts suggest the existence of two density waves sliding with a fast velocity and a slow one in the adjacent domains.[26] When the slow SDW generating a peak at $f_1=f-f'$ in NBN spectrum interacts and interferes strongly with the fast SDW generating a peak at f, we may observe two peaks with frequencies of $f+f'=2f-f_1$ and $f'=f-f_1$. The slow SDW is almost incoherent because the peaks at f' and $f\pm f'$ are weak and broad, while the fast SDW is more coherent. Especially, not only when the velocity of the fast SDW is close to that of the slow SDW but also when the latter is approximately $1/2$ or $2/3$ times the former, the interference is strong. Thus, the fast SDW slides more slowly, while the slow SDW slides more rapidly. At $I=0.27$ and 0.275 mA the weak peak at f_1 sharpens and increases in intensity, approaching the fundamental peak at f. The SDWs with slower velocities gradually are joined in the coherent SDW at a high speed. Finally, the combined peak grows as a fundamental peak of the periodic peaks and sharpens quickly with increasing I above I_2.

Moreover, many sidebands with a periodicity of f' appear around the fundamental and the harmonics just above I_2, i.e., at $I=0.28$, 0.285, and 0.29 mA. In order to see the weak periodic sidebands more clearly, we show a typical case when $I=0.28$ mA in Fig. 9.

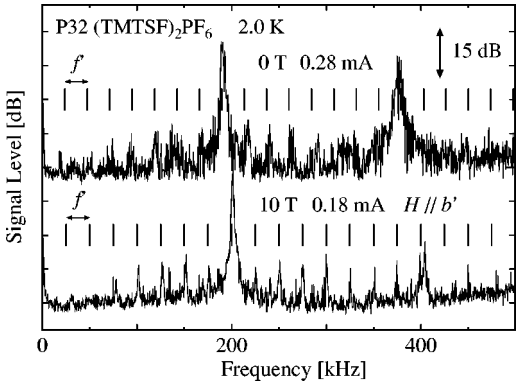

FIG. 9. NBN spectra of sample P32 when $I=0.28$ mA and $H=0$ T and when $I=0.18$ mA and $H=10$ T. f' represents the interval frequency of the periodic sidebands and the two cases hold that $f'=f/8$.

The interval frequency f' of the weak periodic sidebands is equal to f/p, where f is the fundamental frequency of the strong periodic peaks and p is an integer. The case of $I=0.28$ mA in Fig. 9 stands for $f'=f/8(p=8)$, and the cases of $I=0.285$ and 0.29 mA stand for $p=7$ and 6, respectively. This indicates existence of two density waves with almost the same velocity, which are interfering strongly with each other. Far above I_2 the periodic sidebands around the strong periodic peaks disappear. Probably, the SDWs moving with various velocities begin to slide coherently at a uniform speed all over the sample above I_2, because the observed periodic peaks quickly sharpen with increasing I. However, the current dependence of the frequency is contrary to Eq. (1). And, the current oscillation changes from the saw-toothed wave to the bipolar-pulse-type wave, as shown in Fig. 7(b). Moreover, the periodic peaks weaken in intensity at large currents.

We briefly summarize in sample P32 that the SDW slides with plastic deformations, resulting in spatially nonuniform dc currents. At large currents the SDW begins to move coherently in the whole sample.

D. Magnetic-field effects

Similar NBN spectra were obtained in sample P32 when a magnetic field of 10 T was applied along the b' axis, as shown in Fig. 10(a). The current oscillations calculated by the inverse Fourier transformation are also shown in Fig. 10(b). The b' axis is approximately parallel to the easy axis of magnetization b^*.[27] Although the energy band is split by the Zeeman effect when a magnetic field is applied, the nesting of the Fermi surface remains unchanged in pure SDW.[28] On the other hand, when the magnetic field was applied along the c^* axis, the field-induced SDW was observed. It is due to the fact that the Fermi surface becomes more one-dimensional by the application of magnetic field.[29] It should be noted that the present magnetic effect does not come from the well-known fact of the change in the nesting responsible

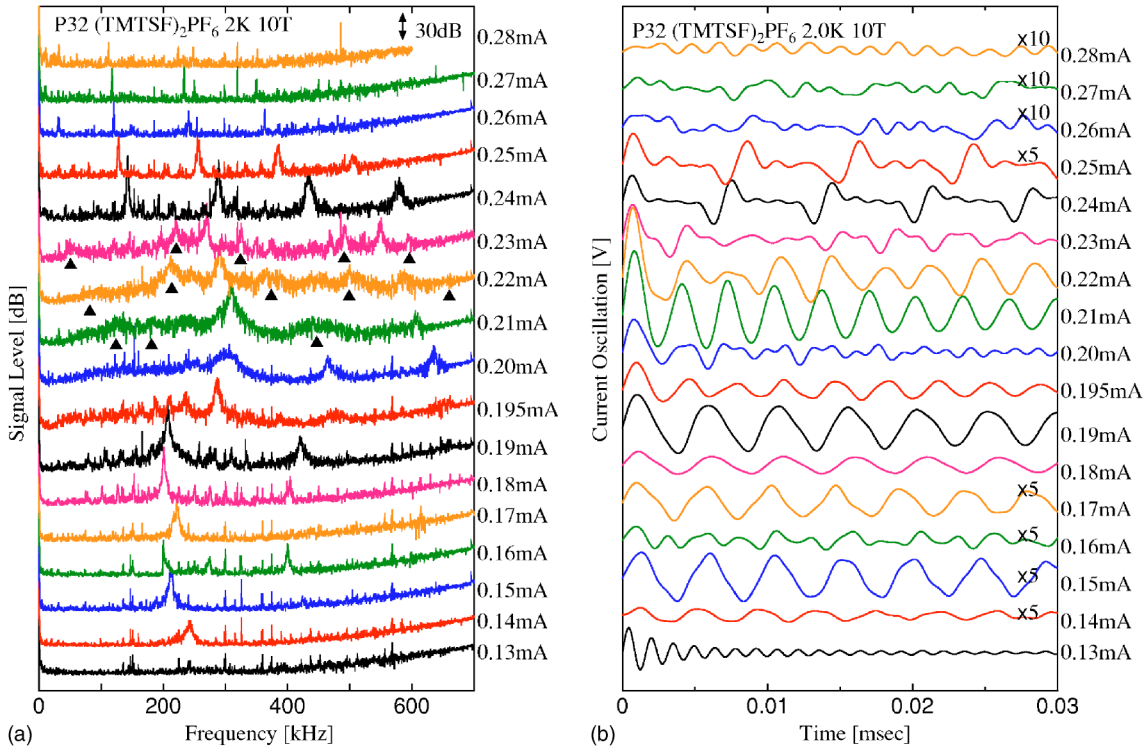

FIG. 10. (Color online) (a) NBN spectra of sample P32 at 2 K when $H=10$ T and (b) the current oscillations obtained by the inverse Fourier transformation. Triangles denote the weak peaks. The current oscillations were obtained by subtracting those at 0.13 mA. The oscillation at 0.13 mA originates from the limited frequency region in the measurements.

for the field-induced SDW by the application of magnetic field.

All the spins are canted at 10 T, because the applied magnetic field is higher than the spin-flop critical field $H_c \cong 0.45$ T, but the magnetization is not saturated yet.[27,30] The NBN spectra were observed even when all the spins were canted.

However, the region from $I_1(\simeq 0.193$ mA) to $I_2(\simeq 0.235$ mA), where the NBN spectrum broadened and several weak broad peaks appeared due to the interference between a fast CDW and a slow one, shifted to smaller currents, as shown in Figs. 8(b) and 10(a). The fundamental frequency jumped at I_1 and I_2. The periodic sidebands with a regular interval frequency f' were observed near I_1 and I_2. A typical case of $I=0.18$ mA at 10 T, shown in Fig. 9, holds that $f'=f/8$, where f is the fundamental frequency of the strong periodic peaks. The cases of $I=0.19$, 0.24, and 0.25 mA stand for $f'=f/8, f'=f/6$, and $f'=f/5$, respectively. This suggests existence of two density waves sliding with almost the same velocities, and they interact and interfere strongly with each other. The SDWs begin to slide coherently above I_2, and then the frequencies of the strong periodic peaks decrease with increasing I. The current dependence of the fundamental frequency below I_1 fits an extrapolated line obtained from that above I_2, which is denoted by a dashed line in Fig. 8(b). They are linked with each other except for the current region of $I_1 \leqslant I \leqslant I_2$.

IV. DISCUSSION

It has been proposed that the SDW state of $(TMTSF)_2PF_6$ is divided into three subphases: SDW1 between 12 and 3.5 K, SDW2 between 3.5 and 2 K, and SDW3 below 2 K.[31] In NMR studies,[31,32] two anomalies of T_1^{-1} were found at about 3.5 and 2 K besides the SDW transition temperature of 12 K. The corresponding anomalies were observed by heat capacity,[33,34] dielectric constant,[33,35] magnetic susceptibility,[36] and magnetotransport.[37] Recently, Kagoshima *et al.*[12] reported by x-ray measurement that the superlattice reflections due to $2k_F$ and $4k_F$ CDWs disappeared below 3–4 K. They stated that the SDW1 and SDW2 subphases are the coexistent SDW-CDW state, but the amplitude of CDW is very small in the SDW2 subphase. And, the SDW3 subphase is a pure SDW state. Then, the temperature of 2 K where we clearly observed the periodic peaks in the NBN spectra is near the phase-transition temperature between the SDW2 subphase and the SDW3 one. At 4.2 K the periodic peaks were not observed in sample P55.

The observed NBN spectrum of sample P56 in Fig. 2 is a typical one, so-called "stick-slip noise," which has been frequently observed in the case of CDW.[9,20]

The stick-slip noise originates from the saw-toothed wave. The Fourier series of the saw-toothed wave shown in Fig. 11(b) is written as

$$\sum_{\ell=1}^{\infty} \frac{1}{\ell} \sin(2\pi \ell f t). \tag{5}$$

Then, the intensity of the ℓth harmonic of the saw-toothed wave is given as $1/\ell^2$ and agrees with the NBN observed when $I=0.31$ mA in sample P56, as shown in Fig. 11(a), although the intensities of the harmonics at $\ell \geqslant 4$ deviate

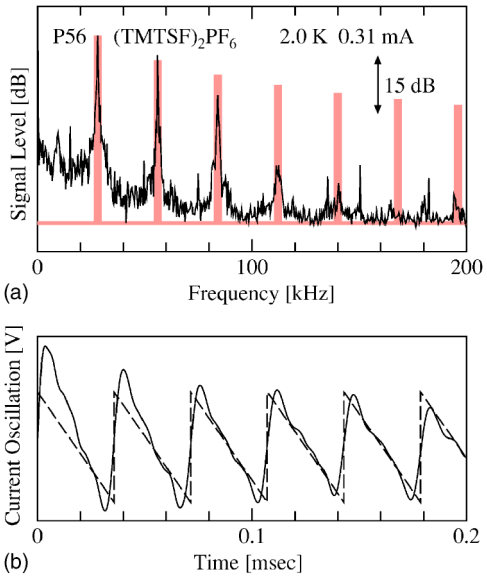

FIG. 11. (Color online) (a) Comparison between the NBN spectra of sample P56 when $I=0.31$ mA and the Fourier components (light brown bars) of the saw-toothed wave given as Eq. (5), and (b) the current oscillation calculated from the NBN spectrum (solid line) and the saw-toothed wave (dashed line).

largely from $1/\ell^2$. Of course, the current oscillations by the inverse Fourier transformation exhibit the saw-toothed wave, as seen in Fig. 11(b). Littlewood[38] showed in the numerical simulations for the sliding CDW that the motion of the CDW occurred via local jumps of a wavelength at impurity sites in the sample when the deformable CDW was pinned by random impurities in applied electric fields greater than E_T, i.e., the deformable CDW slides like as an inchworm does. The saw-toothed wave observed in the present experiment probably comes from similar motions of the deformable SDW.

In classical dynamics the stick-slip motion under dry friction is well known. The stick-slip motion is observed when the kinetic friction coefficient decreases with increasing velocity in the low-velocity region.[39] The current oscillations showing the saw-toothed wave correspond to the stick-slip motion.

In sample P55 we observed the stick-slip noise, whose fundamental frequency is written as Eqs. (1) and (4), in the whole current region. In addition to it, we found the abnormal periodic peaks whose frequencies decreased with increasing I. This is quite unusual behavior. Usually the peak frequency of the NBN increases as the current I is increased. At $I_1' \leqslant I \leqslant I_2'$, the abnormal periodic peaks are split from the second, fourth, and sixth harmonics of the stick-slip noise. A possible explanation is given in terms of the existence of a density wave with a $4k_F$ wave number. As will be discussed later in detail, other possibilities, e.g., effects of the temperature rise of the sample due to the joule heating and the decrease of I_{SDW} in a narrow part of the sample when the total current I is increased will be excluded. The decrease of the frequency with current indicates that the velocity of the $4k_F$-density wave equal to the $2k_F$ SDW gradually decreases with increasing I above I_1'. We think that it is evidence for the existence of the collective mode of the $4k_F$-density wave in the SDW state.

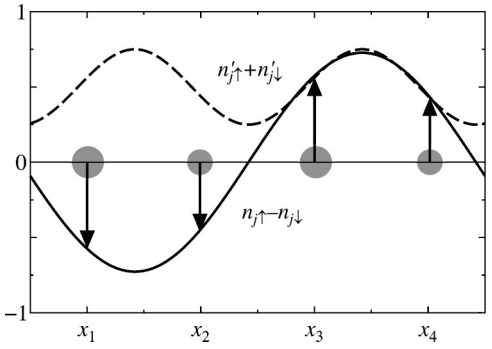

FIG. 12. The schematic diagram for the coexistent state of $2k_F$ SDW and $4k_F$ CDW near pure SDW state. The solid and dotted lines denote $2k_F$ SDW and $4k_F$ CDW, respectively. Arrows denote the magnitudes of the spin at the TMTSF-molecule sites, and circles those of the charge density.

On the other hand, the splitting of the stick-slip noise at $I_1' \leqslant I \leqslant I_2'$ suggests that a part of the $2k_F$ SDW moves with a fast velocity and almost the remaining part of the $2k_F$ SDW moves with a slow velocity which fits Eq. (1). The appearance of the $2k_F$ SDW with a fast velocity strongly correlates with the $4k_F$-density wave sliding slowly.

The phase boundary between the SDW2 and the SDW3 subphases lies around 2 K, and the amplitudes of the $2k_F$ and $4k_F$ CDWs are considered to be small at 2.0 K. There are two dimers of TMTSF molecule in a unit cell of the SDW state of $(\mathrm{TMTSF})_2\mathrm{PF}_6$. Neglecting the effect of the $2k_F$ CDW, the coexistent state $(\downarrow\downarrow\uparrow\uparrow)$ of $2k_F$ SDW and $4k_F$ CDW, which is near the pure SDW state $(\downarrow\downarrow\uparrow\uparrow)$,[14–18,40] is schematically drawn in Fig. 12.

Suzumura and his co-worker[17–19] studied theoretically the collective modes in the one-dimensional quarter-filled SDW states and pointed out that the phase mode at long wavelength is coupled with the $4k_F$-CDW fluctuations even in pure SDW state. Thus, the sliding mode of the $2k_F$ SDW is accompanied by $4k_F$ CDW. Then, it is probable that the $4k_F$ CDW has a phase degree of freedom and it follows $2k_F$ SDW. We think that the abnormal fundamental and harmonic peaks whose frequencies decrease with increasing I arise from the sliding mode of the $4k_F$ CDW.

The spin density at the jth TMTSF-molecule site x_j along the a axis in the $2k_F$ SDW state accompanied by $4k_F$ CDW is described by[17,18]

$$n_{j\uparrow} - n_{j\downarrow} = 2A \sin(2k_{Fx}x_j + \theta), \tag{6}$$

and the $4k_F$-electron density with spin σ is described by

$$n'_{j\sigma} = \tfrac{1}{4} - C\cos(4k_{Fx}x_j + \theta'). \tag{7}$$

Here, $2C$ is the amplitude of the $4k_F$ CDW. Below $I_1'=9.0$ mA the $4k_F$ CDW slides with the same velocity as the $2k_F$ SDW does, i.e.,

$$\frac{d\theta}{dt} = \frac{1}{2}\frac{d\theta'}{dt} = 2k_{Fx}v_{\mathrm{SDW}} = \frac{2\pi}{\lambda_{\mathrm{SDW}}}v_{\mathrm{SDW}}. \tag{8}$$

They keep the mutual phase difference constant in sliding. It is feasible that the $2k_F$ SDW and $4k_F$ CDW move with dif-

ferent velocities. Thus, above I_1' the velocity (v_{CDW}) of the $4k_F$ CDW becomes slower than that (v'_{SDW}) of the $2k_F$ SDW. Their mutual phase relation changes as time passes. It is probably due to existence of the impurity centers, which play different roles in the pinning mechanism between CDW and SDW, and the difference becomes conspicuous when they move with fast velocities.

The $2k_F$ SDW is sliding faster than when it slides together with the $4k_F$ CDW at the same velocity v_{SDW}, i.e., $v'_{SDW} > v_{SDW}$, so that the total currents carried are equal to those when they move with the same velocity. Then, we observed that a SDW was sliding with a fast velocity along a bundle of the one-dimensional chains and another SDW was sliding with a slow velocity along another bundle of the chain at $I_1' \leqslant I \leqslant I_2' = 12.0$ mA in sample P55. In the latter part the $2k_F$ SDW slides together with the $4k_F$ CDW at the same velocity v_{SDW}.

Above I_2' the abnormal peak turns to increase in frequency with increasing I, and then the frequency is approximately equal to 3/2 times the fundamental frequency of the stick-slip noise. Moreover, we observed a weak peak at a half of the fundamental frequency. This fact suggests that the $2k_F$ SDW at a speed of $v'_{SDW}(\sim v_{SDW})$ and the $4k_F$ CDW at a speed of $v'_{SDW}/2$ interact strongly and interfere with each other. Using Eqs. (6) and (7) and $\theta' = \theta + \gamma_0$ (γ_0 is a constant), this interference generates the following waves:

$$(n_{j\uparrow} - n_{j\downarrow}) + \left(n'_{j\uparrow} + n'_{j\downarrow} - \tfrac{1}{2}\right) = 2(A + C)\sin(2k_{Fx}x_j + \theta) - 4C\cos(k_{Fx}x_j + \gamma) \times \sin(3k_{Fx}x_j + \theta + \gamma), \quad (9)$$

where $\gamma = \gamma_0/2 + \pi/4$. The $3k_F$ density wave described by the second term in Eq. (9), which stands for the relation of $d\theta/dt = 3k_{Fx}v'_{SDW}$, generates a peak at about 3/2 times the fundamental frequency of the stick-slip noise in the NBN spectrum.

The weak periodic peaks with a half of the periodicity probably are expected to appear owing to the higher-order interference.

We think that this interference gives a strong piece of evidence of the $4k_F$ density wave, because a $2k_F$ SDW sliding at a speed of $2v_{SDW}$ could not generate a peak at about 3/2 times the fundamental frequency of the stick-slip noise, i.e., $\sim 3f/2$, in an interference. If the $2k_F$ SDW sliding at a speed of $2v_{SDW}$ slowed its speed down to $\sim v_{SDW}$, the interference between two $2k_F$ SDWs with almost the same velocities induced the appearance of many sidebands with a periodicity of f/p, as seen in sample P32 in Fig. 9.

These results suggest the existence of the internal distortions and of the collective mode of the $4k_F$ CDW in the SDW of $(TMTSF)_2PF_6$. Moreover, the SDW is deformable and not coherent in the whole sample, i.e., there is a possibility that the SDWs slide with different velocities in different domains.[26]

In sample P32 the NBN spectra are very complicated. The frequency of the fundamental increases with increasing I below $I_1 \simeq 0.245$ mA at 0 T, and the current oscillations exhibit the saw-toothed wave due to the stick-slip noise. We estimated $\lambda_{pin} = 1.3$ Å but it is much shorter than $\lambda_{SDW} \simeq 14.6$ Å. This suggests that the observed spectra come from the SDW sliding fast, but we could not observe slow SDWs because they were incoherently sliding. In fact, the fundamental peak shifted largely when I was increased from 0.2 to 0.21 mA, and the weak remainder, denoted by a closed triangle in Figs. 7(a) and 8(a), remained observable at the same frequency. This suggests that there are several SDWs sliding with various velocities in sample P32. At $I_1 \leqslant I \leqslant I_2 \simeq 0.278$ mA the coexistence of the fast and slow SDWs interacting and interfering with each other was confirmed, too. We observed a sideband at $f \pm f'$ around the fundamental of the strong periodic peaks and a very weak broad peak at f'. They are generated by interfering between two waves with frequencies of f and $f_1 = f - f'$, i.e., the frequencies $f \pm f'$ of the sideband correspond to $f - f_1$ and $2f - f_1$. The pairs of the sideband approach each other in frequency with increasing I. We also observe a sideband at $2f - f' = f + f_1$ and $2f + f' = 3f - f_1$ around the second harmonic peak at $2f$ in the cases of $I = 0.22$ and 0.23 mA when $H = 10$ T in Figs. 8(b) and 10(a). In general, we suppose that the sidebands appear strongly at $\ell f \pm f_1$. The fast and slow SDWs are sliding in the adjacent domains and generating strong periodic peaks at ℓf and a weak peak at f_1. At the domain-boundary region they superimpose on each other and generate the following current oscillations with frequencies of $\ell f \pm f_1$:

$$A_\ell \sin(2\pi \ell f t) \times A' \sin(2\pi f_1 t + \delta) = -\frac{A_\ell A'}{2}[\cos\{2\pi(\ell f + f_1)t + \delta\} - \cos\{2\pi(\ell f - f_1)t - \delta\}], \quad (10)$$

where δ is the phase difference.

Near I_2 they interact and interfere strongly with each other, together with an intensity transfer from the fundamental of the periodic peaks to the weak broad peak at f_1. The coherency of SDW generating the peak at f_1 grows in the domain with increasing I, because the peak sharpens. Above I_2 the combined peak grows into a fundamental peak of the periodic peaks. At that time, we observed the periodic sidebands at $\ell f \pm mf'$ around the fundamental and the harmonics at ℓf, as shown in Fig. 9, where $m = 1, 2, \ldots, p-1$. These frequencies ($\ell f \pm mf'$) are rewritten as $\{(\ell \pm m)f \mp mf_1\}$. From the experimental result we obtain that $f' = |f - f_1| \simeq 23.7 - 25.8$ KHz and f' hardly changes with increasing I above I_2. Then, this indicates that two density waves almost coherently slide at almost the same velocities in two adjacent domains just below I_2, which interfere strongly with each other. The two domains unite with each other above I_2, and then the interference between the two strong periodic peaks gives rise to lots of sidebands around the strong periodic peaks. The coherency grows rapidly in the whole sample above I_2, and consequently the periodic peaks sharpen. This process averages the velocities of the fast SDW and the slower SDWs and then the velocity of the SDW governing the NBN spectrum is decreased. As a result, the fundamental frequency of the periodic peaks decreases with increasing I. Moreover, the current oscillations change from the saw-toothed wave to the

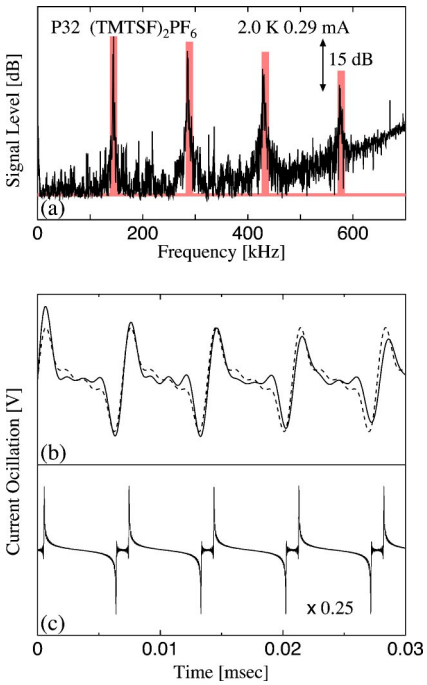

FIG. 13. (Color online) (a) Comparison between the NBN spectrum of sample P32 when $I=0.29$ mA and $H=0$ T and the Fourier components (light brown bars) of the bipolar-pulse-type wave given as Eq. (13) assuming that $\theta_0=0, \phi_0=0.15\pi$, and A_ℓ is independent of ℓ; (b) comparison between the current oscillation calculated from the NBN spectrum (solid line) and the bipolar-pulse-type wave (dotted line) calculated by summing the Fourier components up to $\ell=4$ in Eq. (13), and (c) the bipolar-pulse-type wave calculated by summing the Fourier components up to $\ell=100$ in Eq. (13).

bipolar-pulse-type wave, which is shown in the typical case of $I=0.29$ mA in Fig. 13.

The sliding motion of the SDW coexisting with the $2k_F$ CDW, which is described by Eqs. (2) and (3), may generate the following current oscillation when $A_\uparrow=A_\downarrow\equiv A$:

$$\sum_{\ell=1}^{\infty} A_\ell\{\sin \ell(2\pi ft+\theta_0+\phi)+\sin \ell(2\pi ft+\theta_0-\phi)\}$$
$$=\sum_{\ell=1}^{\infty} 2A_\ell \cos(\ell\phi)\sin \ell(2\pi ft+\theta_0). \quad (11)$$

The present NBN spectra were observed in the narrow temperature region near 2 K. This temperature region lies at the boundary between the SDW2 and SDW3 subphases. The SDW2 subphase is the coexistent SDW-CDW state but the amplitude of CDW is very small, and the SDW3 subphase is a pure SDW state. Thus, the static part of CDW coordinate $\overline{\phi}$ may be regarded as zero. On the other hand, Tomio and Suzumura[17] theoretically studied the collective modes of the SDW in a one-dimensional electron system with a quarter-filled band by the extended Hubbard model, taking into consideration the next-nearest-neighbor interaction V_2. They indicated that the CDW excitation with a low energy existed even at pure SDW state near the phase boundary of the coexistent SDW-CDW state, and the gap in the CDW excitation spectrum vanished at a critical value of V_2 corresponding to the phase boundary.

This low-energy ($\hbar\omega_0$) CDW collective excitation mode, which is described by the dynamical part of ϕ

$$\delta\phi=\phi_0 \sin \omega_0 t, \quad (12)$$

can also contribute to the nonlinear transport phenomena. Here, ϕ_0 is the amplitude of the CDW excitation. Then, the intensity of the ℓth harmonic of the NBN is given as

$$\sum_{\ell=1}^{\infty} 2A_\ell\left\{\frac{1}{T}\int_0^T \cos(\ell\phi_0 \sin \omega_0 t)dt\right\}\sin \ell(2\pi ft+\theta_0)$$
$$\cong \sum_{\ell=1}^{\infty} 2A_\ell J_0(\ell\phi_0)\sin \ell(2\pi ft+\theta_0), \quad (13)$$

where T is the time of observation and J_0 is the zeroth-order Bessel function.

Assuming that the coefficient A_ℓ is independent of ℓ, the calculated current oscillation is displayed in Fig. 13(b), when the Fourier components are summed up to $\ell=4$. It agrees well with that obtained by the present experiment when $I=0.29$ mA. If we measure the NBN spectrum by much higher frequency, the current oscillation should correspond to that shown in Fig. 13(c), in which the Fourier components were summed up to $\ell=100$ in Eq. (13). At present we think that the NBN spectra at large currents come from the sliding $2k_F$ SDW together with the $2k_F$-CDW excitation. Since the frequency of $2k_F$-CDW excitation is low in the vicinity of the phase boundary between the SDW2 and SDW3 subphases, the NBN spectra due to the CDW excitation were able to be detected around 2 K. These facts lead to the point that not only the phason but also the $2k_F$-CDW excitation plays important roles in carrying the nonlinear current at large currents.

At $I_1 \leqslant I \leqslant I_2$ the NBN spectrum drastically changes, which suggests that a dynamical phase transition occurs. Balents and Fisher[41] and their co-workers[42] studied theoretically the dynamical phase transition from the plastic-flow phase, which consists of spatially nonuniform dc current, to the moving-solid phase with coherent elastic flow as the velocity of a driven CDW state is increased. In the moving-solid phase, despite the absence of true spatial long-range order and periodicity, the CDW has long-range temporal correlation. Recently this dynamical phase transition was observed in the sliding CDW state of TaS_3.[43] In the vortex lattice of type II superconductor a similar dynamical phase transition was theoretically studied by Koshelev and Vinokur,[44] and it was observed in Nb and $NbSe_2$ by neutron diffraction.[45–47] In the present SDW state, there exists not only a sliding degree of freedom θ but also a degree of freedom for the relative motion ϕ. Although this dynamical phase transition cannot be simply applied to the present SDW state, we think that a similar dynamical phase transition occurred at I_2. The NBN spectra at $I_1 \leqslant I \leqslant I_2$ are due to the precursor of the phase transition when $H=0$ T. As stated before, the SDW sliding at a high speed in a part of the sample is almost coherent, while the CDWs in the remaining part with lower velocities are incoherent. Then, the observed

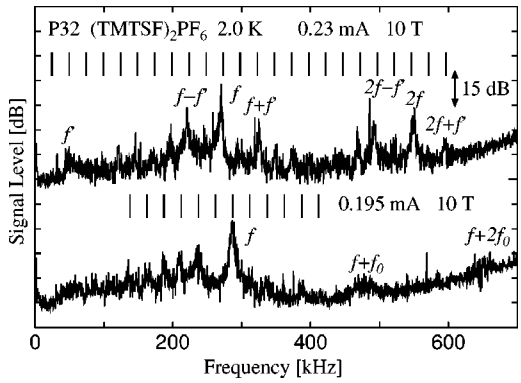

FIG. 14. NBN spectra of sample P32 when $I=0.195$ mA and $H=0$ T and when $I=0.23$ mA and $H=10$ T.

periodic peaks come from the former, and consequently their fundamental frequency is much higher than the expected value of Eq. (1). After the dynamical phase transition at I_2 the coherency grew rapidly in the whole sample and then the periodic peaks became very sharp. Simultaneously, the observed fundamental frequency decreased with increasing I and approached quickly the expected value of Eq. (1). Moreover, the relative motion also became coherent, and we were able to detect the $2k_F$-CDW excitation.

When the magnetic field is applied along the b' axis all the spins are canted. The magnetic field probably helps to grow the coherency in the SDW state, which decreased the current region between I_1 and I_2 where the nonperiodic broad peaks appeared due to the interference, i.e., the dynamical phase transition took place at small current. However, the current dependence of the fundamental frequency of the periodic peaks below I_1 fits the extrapolated line obtained by the current dependence above I_2, as seen in Fig. 8(b). The state observed below I_1 is regarded as a quasi-elastic-flow state, but it is unstable. In this current region, the plastic-flow state competes with the quasi-elastic-flow state, and the former appears between I_1 and I_2.

We expand the NBN spectra at 0.195 mA ($\sim I_1$) and 0.23 mA ($\sim I_2$) when $H=10$ T in Fig. 14. When $I=0.195$ mA the strongest peak appeared at $f=286$ KHz. We also observed two weak peaks at about 473 and 656 KHz, which do not correspond to $2f$ and $3f$, i.e., they are not the second and third harmonics. Their frequencies are written as $f+f_0$ and $f+2f_0$, where f_0 ($\sim$185 KHz) fits the extrapolated line denoted by the dashed line in Fig. 8(b). Moreover, we observed periodic sidebands around the main peak at $f=286$ KHz below 400 KHz. Thus, this state at $I=0.195$ mA is regarded as a mixed state of the plastic-flow state and the quasi-elastic-flow one. Surprisingly, at $I=0.20$ mA, i.e., just above I_1, f_0 approaches $f/2$ owing to the mutual adjustment in their velocities and then the peak at $f+2f_0$ may be regarded as the second harmonic of $2f$.

At 0.23 mA ($\sim I_2$) we observed a sideband at $f\pm f'$ around the main peak at f and a very weak peak at $f'=f-f_1$ due to the interference between the two waves with f and f_1, as mentioned above. We notice other several weak peaks possessing a periodicity of $f'/2=(f-f_1)/2$, which corresponds to $f/11$. Probably the mutual adjustment works on their velocities, and consequently f_1/f becomes a commensurate value ($=9/11$). We think that the appearance of the periodic sidebands at $I=0.23$ mA represents a precursor of the phase transition from the plastic-flow state to the elastic-flow one. Taking into consideration the frequency jump of the main peak at I_1 and I_2 in addition to the above-mentioned facts, the phase transitions are a first-order type.

Just below I_1 and just above I_2 we observed weak periodic sidebands around the strong periodic peaks (the typical case is shown in Fig. 9), indicating the strong interference between the sliding SDWs at almost the same speed in a combined domain. The coherency grows rapidly in the whole sample, and then the moving-solid phase is formed in the sliding SDW state when I goes beyond I_2.

The NBN spectra reported here were measured under constant electric currents. Self-heating by the joule heat may be a problem in all such measurements with constant currents. We observed the unusual periodic peaks at $I_1' \leqslant I \leqslant I_2'$ in sample P55 and at $I \geqslant I_2$ in sample P32, whose frequencies decreased with increasing current in the large current regions. The fundamental frequency f of the periodic peaks in the NBN is independent of temperature, assuming that the density of condensed electron n_{SDW} does not change. Nomura *et al.*[6] observed that the peak did not change in frequency but broadened with increasing temperature in the NBN of $(TMTSF)_2ClO_4$. When the temperature is increased towards the critical temperature, n_{SDW} is expected to decrease, resulting in the increase of the fundamental frequency f, as written in Eq. (1). It is contrary to the current dependence of the unusual peaks in frequency. Moreover, we observed that the periodic peaks including the abnormal periodic peaks are very sharp at $I_1' \leqslant I \leqslant I_2'$ in sample P55. In sample P32 the periodic peaks sharpen with increasing current above I_2.

Kang *et al.*[4] reported that the threshold electric field E_T was constant below 4.2 K and it increased as the temperature was increased above 4.2 K in most pure $(TMTSF)_2PF_6$ samples. The increase of E_T reduces I_{SDW}, leading to a decrease of the peak frequency of the NBN spectrum. However, we observed no indication of increase of E_T in the $I-V$ characteristic of sample P32 in Fig. 1. The nonlinear current very rapidly increased above a threshold voltage V_T without a marked increase of the applied voltage V, implying that V_T does not change as the total current I is increased, taking into account that sample P32 is very homogeneous and possesses a homogeneous E_T distribution, as discussed in Sec. III C. The result of the $I-V$ characteristic and the sharpening of the abnormal periodic peaks with current above I_2 denies the effect of the temperature rise by the joule heating in sample P32.

Unfortunately, we did not measure the $I-V$ characteristic of sample P55 in the region where the abnormal periodic peaks were found. If the threshold electric field E_T changes, the fundamental frequency f of the stick-slip noise does not linearly increase as a function of J_{SDW}. However, f of the stick-slip noise fits well with Eqs. (1) and (4) even at large currents in sample P55, suggesting that the E_T did not change. Kang *et al.*[4] reported that E_T was constant below 4.2 K and our experimental result showed that the NBN peaks were not observed at 4.2 K. These facts support that the E_T

did not increase as I was increased in sample P55.

Lyding *et al.*[48] studied NBN in the CDW system of $NbSe_3$ in the presence of a thermal gradient, and they observed multiple splitting of the noise peaks with increasing temperature gradient. In this case the periodicity of the splitting peaks should be broken in contrast with the unusual periodic peaks observed in the present experiments. Of course, it is impossible to give rise to temperature gradient so as to keep the average temperature unchanged. Then, the appearance of the unusual periodic peaks does not originate from the temperature rise and gradient.

In organic materials the sample cracking is difficult to avoid in the cooling process, which may lead to nonuniform current flows. Moreover, when the distribution of the threshold electric field E_T is inhomogeneous in the sample, different excess currents I_{SDW} which are carried by the SDW condensates may flow in different parts of the sample. Then, the current density J_{SDW} carried by the SDW condensate might decrease in a part of the sample even when the total current I is increased, leading to the unusual dependence of the NBN frequency on the total current. On the other hand, as mentioned before, the $I-V$ characteristic suggests that the distribution of the threshold electric field E_T is very homogeneous in the whole of sample P32. Then, sample P32 has a homogeneous resistivity ρ, neglecting the intrinsic domain structure of the sliding SDW state. Since $V=\rho JL$, where J is the current density flowing in the part of the sample with resistance R in the circuit of Fig. 4(a) and L is its length, the measured voltage V is independent of the cross section of the part of the sample in which the NBN were measured. In the $I-V$ characteristic of sample P32, the total current I was increased by applying an almost constant voltage $V\cong V_T$. There is no possibility of J_{SDW} decreasing under the almost constant V in the homogeneous samples even if the fraction of the sample cross section carrying the SDW current is changed. Moreover, under a magnetic field of 10 T the decrease of the frequencies of the NBN peak with current was observed even at small currents, suggesting that this phenomenon is intrinsic.

The $I-V$ characteristic of sample P55 suggests that the threshold electric fields E_T are widely distributed all over the sample. Several series of the fundamental and harmonics were observed in the NBN spectra of the inhomogeneous CDW systems.[21–24] This is due to the fact that the electric field component along the chains is inhomogeneous and different currents flow in the different parts of the sample.[24] However, all the frequencies of the NBN peaks reported there increased with increasing current. As far as we know, there is no report that the NBN peaks decrease in frequency as the total current I is increased. Moreover, in order to explain the abnormal peak of sample P55 in terms of the decrease of J_{SDW} flowing in a part of the sample, it is necessary to consider the SDW sliding at a speed of just twice the velocity of the usual SDW below I_1'. It is, however, very difficult to interpret the peak at about $3/2$ times the fundamental frequency of the stick-slip noise above I_2' in terms of the coexistence of $2k_F$ SDWs with almost the same velocities. As stated before, the appearance of the peak at about $3f/2$ can be interpreted by the interference between $4k_F$-density wave and $2k_F$ SDW. At present we think that this interference gives a strong piece of evidence for the coexistence of the collective mode of $4k_F$-density wave in the SDW state.

V. CONCLUSION

We studied narrow-band noise (NBN) in the SDW state of $(TMTSF)_2PF_6$. Typical NBN spectra coming from the sawtoothed-wave current oscillations were clearly observed, which is understood in terms of the stick-slip motion in classical dynamics. Moreover, we obtained evidence of the existence of the $4k_F$-CDW collective excitation together with the coexistence of the $2k_F$ SDWs with a fast velocity and a slow one. This fact indicates that the $4k_F$-CDW fluctuations accompany the phason mode at long wavelength. Spatially nonuniform dc currents are carried by the deformed SDW. The fast SDW generating sharp periodic peaks in the NBN spectrum and the slow SDW in another adjacent domain interfere with each other, resulting in emergence of the weak broad sidebands around the main periodic peaks. The peak of the slow SDW is very broad, indicating that it is almost incoherent. At large currents, the NBN spectrum largely changed with increasing current and depends on applied magnetic field, suggesting a dynamical phase transition from the plastic-flow phase to the moving-solid phase. In the moving-solid phase the frequencies of the periodic peaks decreased with increasing current, because the spatial coherency grew all over the sample, and consequently the fundamental frequency f decreases and approaches the expected value given by Eq. (1). The bipolar-pulse-type waves were observed in the current oscillations at this phase, which is interpreted in terms of the coexistence of the $2k_F$-CDW collective excitation with the phason mode in the SDW state. The coherency of the SDW is developed by the application of magnetic field along the b' axis, resulting in the competing between the plastic-flow phase and the moving-solid phase at small currents.

ACKNOWLEDGMENTS

We are grateful to Professor T. Takahashi for providing us with samples. We also thank Professor Y. Suzumura and Dr. Y. Tomio for helpful discussion.

*Electronic address: t-sekine@sophia.ac.jp

[1] P. Monceau, N. P. Ong, and A. M. Portis, Phys. Rev. Lett. **37**, 602 (1976).
[2] S. Tomić, J. R. Cooper, D. Jérome, and K. Bechgaard, Phys. Rev. Lett. **62**, 462 (1989).
[3] W. Kang, S. Tomić, J. R. Cooper, and D. Jérome, Phys. Rev. B **41**, 4862 (1990).
[4] W. Kang, S. Tomić, and D. Jérome, Phys. Rev. B **43**, 1264 (1991).
[5] K. Nomura, T. Shimizu, K. Ichimaru, T. Sambongi, M. Tokumoto, H. Anzai, and N. Kinoshita, Solid State Commun. **72**, 1123 (1989).
[6] K. Nomura, N. Keitoku, T. Shimizu, T. Sambongi, M. Tokumoto, N. Kinoshita, and H. Anzai, J. Phys. IV Suppl. I, **3** 21 (1993).
[7] G. Kriza, G. Quirion, O. Traetteberg, W. Kang, and D. Jérome, Phys. Rev. Lett. **66**, 1922 (1991).
[8] N. Hino, T. Sambongi, K. Nomura, M. Nagasawa, M. Tokumoto, H. Anzai, N. Kinoshita, and G. Saito, Synth. Met. **40** (1991) 275.
[9] For example, see G. Grüner, in *Density Waves in Solids* (Addison-Wesley, New York, 1994).
[10] J. P. Pouget and S. Ravy, J. Phys. I **6**, 1501 (1996).
[11] J. P. Pouget and S. Ravy, Synth. Met. **85**, 1523 (1997).
[12] S. Kagoshima, Y. Saso, M. Maesato, R. Kondo, and T. Hasegawa, Solid State Commun. **110**, 479 (1999).
[13] T. Takahshi, Y. Maniwa, H. Kawamoto, and G. Saito, Physica B **143**, 417 (1986).
[14] N. Kobayashi and M. Ogata, J. Phys. Soc. Jpn. **66**, 3356 (1997).
[15] N. Kobayashi, M. Ogata, and K. Yonemitsu, J. Phys. Soc. Jpn. **67**, 1098 (1998).
[16] S. Mazumdar, S. Ramasesha, T. T. Clay, and D. K. Cambell, Phys. Rev. Lett. **82**, 1522 (1999).
[17] Y. Tomio and Y. Suzumura, J. Phys. Soc. Jpn. **70**, 2884 (2001).
[18] Y. Tomio, Thesis (2003).
[19] Y. Suzumura, J. Phys. Soc. Jpn. **66**, 3244 (1997).
[20] R. M. Fleming and C. C. Grimes, Phys. Rev. Lett. **42**, 1423 (1979).
[21] N. P. Ong and C. M. Gould, Solid State Commun. **37**, 25 (1980).
[22] P. Monceau, J. Richard, and M. Renard, Phys. Rev. Lett. **45**, 43 (1980).
[23] J. Richard, P. Monceau, and M. Renard, Phys. Rev. B **25**, 948 (1982).
[24] N. P. Ong and G. Verma, Phys. Rev. B **27**, 4495 (1983).
[25] S. Takada, J. Phys. Soc. Jpn. **53**, 2193 (1984).
[26] J. B. Sokoloff, Phys. Rev. B **31**, 2270 (1985).
[27] K. Mortensen, Y. Tomkiewicz, and K. Bechgaard, Phys. Rev. B **25**, 3319 (1982).
[28] R. H. Mckenzie, cond-mat/9706235.
[29] For example, P. M. Chaikin, J. Phys. I **6**, 1875 (1996).
[30] K. Mortensen, Y. Tomkiewicz, T. D. Schultz, and E. M. Engler, Phys. Rev. Lett. **46**, 1234 (1981).
[31] T. Takahashi, T. Harada, Y. Kobayashi, K. Kanoda, K. Suzuki, K. Murata, and G. Saito, Synth. Met. **41–43**, 3985 (1991).
[32] K. Nomura, Y. Hosokawa, T. Sekibuchi, S. Takahashi, J. Yamada S. Nakatsuji, and H. Anzai, Synth. Met. **86**, 1951 (1997).
[33] J. C. Lasjaunias, K. Biljaković, F. Nad', P. Monceau, and K. Bechgaard, Phys. Rev. Lett. **72**, 1283 (1994).
[34] J. C. Lasjaunias, K. Biljaković, and P. Monceau, Phys. Rev. B **53**, 7699 (1996).
[35] F. Nad', P. Monceau, and K. Bechgaard, Solid State Commun. **95**, 655 (1996).
[36] N. Matsunaga, H. Takashige, K. Keitoku, M. Nagasawa, K. Nomura, and T. Sambongi, Physica B **194–196**, 1265 (1994).
[37] S. Uji, J. S. Brooks, M. Chaparala, S. Takasaki, Y. Yamada, and H. Anzai, Phys. Rev. B **55**, 12 446 (1997).
[38] P. B. Littlewood, Phys. Rev. B **33**, 6694 (1986).
[39] For example, F. Heslot, T. Baumberger, B. Perrin, B. Caroli, and C. Caroli, Phys. Rev. E **49**, 4973 (1994).
[40] H. Seo and H. Fukuyama, J. Phys. Soc. Jpn. **66**, 1249 (1997).
[41] L. Balents and M. P. A. Fisher, Phys. Rev. Lett. **75**, 4270 (1995).
[42] L.-W. Chen, L. Balents, M. P. A. Fisher, and M. C. Marchetti, Phys. Rev. B **54**, 12 798 (1996).
[43] K. -i. Matsuda and S. Tanda, Solid State Commun. **113**, 451 (2000).
[44] A. E. Koshelev and V. M. Vinokur, Phys. Rev. Lett. **73**, 3580 (1994).
[45] P. Thorel, R. Kahn, Y. Simon, and D. Cribier, J. Phys. (Paris) **34**, 447 (1973).
[46] U. Yaron, P. L. Gammel, D. A. Huse, R. N. Kleiman, C. S. Oglesby, E. Bucher, D. J. Bishop, K. Mortensen, K. Clausen, C. A. Bolle, and F. De La Cruz, Phys. Rev. Lett. **73**, 2748 (1994).
[47] U. Yaron, P. L. Gammel, D. A. Huse, R. N. Kleiman, C. S. Oglesby, E. Bucher, D. J. Bishop, K. Mortensen, and K. Clausen, Nature (London) **376**, 753 (1995).
[48] J. W. Lyding, J. S. Hubacek, G. Gammie, and R. E. Thorne, Phys. Rev. B **33**, 4341 (1986).